iScience

CellPress
OPEN ACCESS

Article

The sustainable production of succinic anhydride from renewable biomass

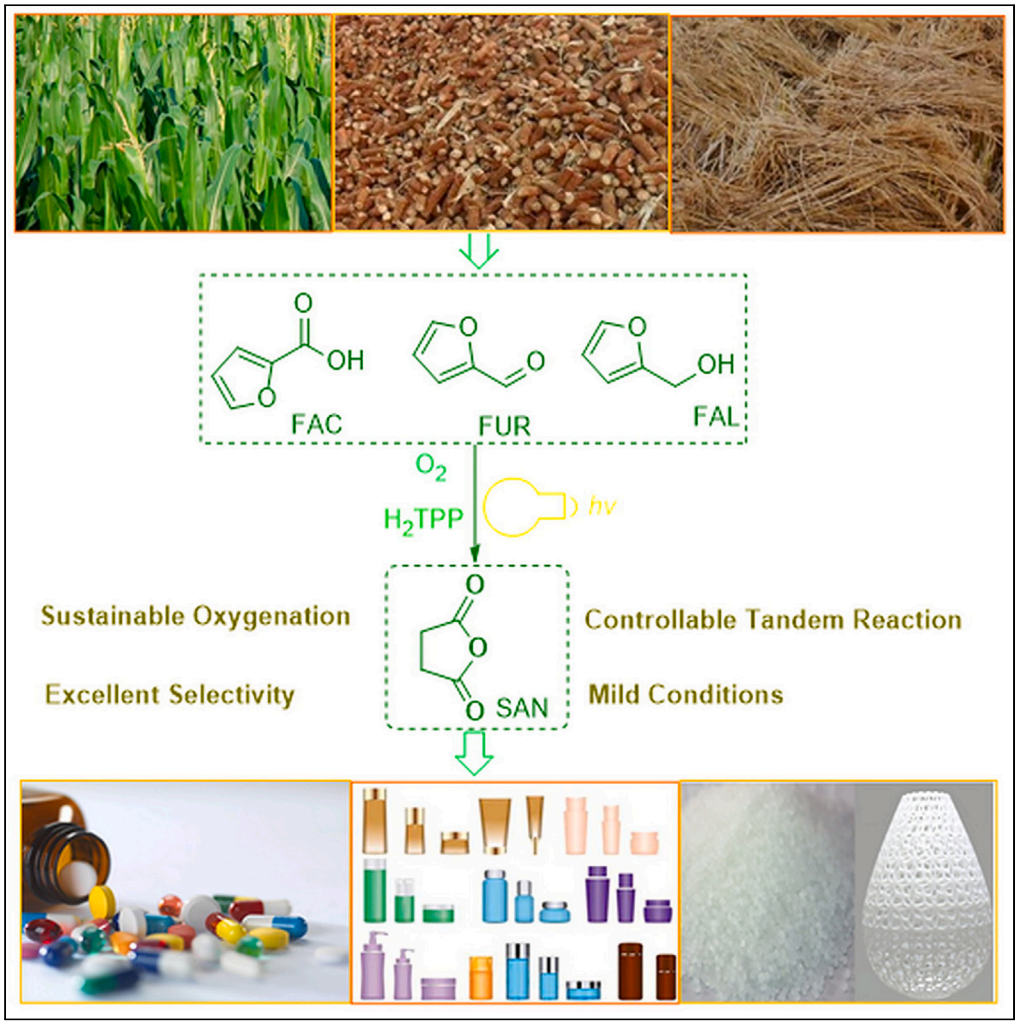

Xiaoqian Gao, Xinli Tong, Yi Zhang, Song Xue

tongxinli@tju.edu.cn

Highlights

A new mode for producing C4 bulk chemicals from biomass

Selective transformation of furans to succinic anhydride (SAN)

Photocatalytic controllable tandem reaction at room temperature

Gao et al., iScience *26*, 107203
July 21, 2023
https://doi.org/10.1016/j.isci.2023.107203

iScience

CellPress
OPEN ACCESS

Article

The sustainable production of succinic anhydride from renewable biomass

Xiaoqian Gao,[1] Xinli Tong,[1,2,*] Yi Zhang,[1] and Song Xue[1]

SUMMARY

The selective production of C4 bulk chemicals from biomass is significant to replace the traditional method from petroleum resource. In this work, the succinic anhydride (SAN) is directly prepared from bio-based furanic platform compounds utilizing the visible light-induced oxygenation process, in which *m*-tetraphenyl porphyrin (H_2TPP) and molecular oxygen was employed as the photocatalyst and terminal oxidant, respectively. Under optimal conditions, a 99.9% conversion with 97.8% selectivity of SAN was obtained from furoic acid (FAC) at room temperature. Moreover, the transformation of furfural and furfuryl alcohol with this system can also generate SAN, and the product selectivity is controllable by tuning light intensity and time. Furthermore, the EPR detection, isotope labeling, and control experiments exhibited that the generation of singlet oxygen plays a crucial role and 5-hydroxy-2(5H)-furanone is the main intermediate during the reaction. Finally, a possible reaction mechanism for the production of SAN from furanic compound is proposed.

INTRODUCTION

Owing to the gradual depletion of fossil resources and the corresponding environmental pollution with their daily use, the future sustainable development will require numerous greener processes and industrial production from the renewable carbon sources. Considering the sustainability and abundance on the earth, biomass resource is regarded as one of the most promising feedstocks for the future chemical industry.[1–3] So, the efficient strategy for valorization of biomass and biomass-based platform compounds needs to be explored and investigated.[4] Especially, furanic platform compounds such as furfural (FUR) and 5-hydroxymethyl furfural (5-HMF) have received tremendous attention because of their wide applications in the synthesis of value-added chemicals and liquid fuels.[5–7] In a sense, FUR and 5-HMF bridge the gap between the biomass feedstock and the biorefinery industry.[8] In particular, the selective production of C4 bulk chemicals from furanic compounds is very significant and helpful in replacing the traditional preparation of petroleum-based products. In addition, it helps to realize the target of carbon neutrality and the sustainable development of society.

Succinic anhydride (SAN), one of the important C4 chemicals, is widely used in the synthesis of numerous pesticides, medicines, cosmetics, and alkyl resins. Moreover, the tetrahydrofuran, γ-butanolactone and 1, 4-butanediol can be prepared through SAN hydrogenation;[9,10] the reaction of SAN with ammonia solution or Schiff base may produce succinimide or the substituted pyrrolidinones.[11,12] Furthermore, the SAN could be used to generate the polymers[13–15] and ion exchangers.[16,17]

Generally, there are two usual methods for the production of SAN in industry; one is the dehydration of succinic acid and the other is the catalytic hydrogenation of maleic acid (shown in the Figure 1). For the succinic acid dehydration, Fieser found that the reaction could be performed at a temperature of 220 to 270°C in the presence of dehydrating agents.[18] Next, Chen et al.[19] employed $H_3PO_4/Nb_2O_5{\cdot}nH_2O$ as the catalyst to promote the dehydration of succinic acid, in which *ca.* 80% yield of SAN was obtained with cyclohexanone as the solvent. This dehydration process is usually carried out at high temperatures, resulting in high energy consumption and greenhouse gas emission. In the case of the maleic anhydride hydrogenation, the reaction needs to be achieved with the supported transition metal catalysts which include the palladium catalyst,[20,21] nickel catalyst,[22–30] copper catalyst,[31] bimetallic Ni-Pt catalyst,[32] and so on. Compared with the succinic acid dehydration route, the selective hydrogenation of maleic anhydride can reduce the energy consumption by performing reactions using solid catalysts at a relatively low

[1]Tianjin Key Laboratory of Organic Solar Cells and Photochemical Conversion, School of Chemistry and Chemical Engineering, Tianjin University of Technology, No. 391, Binshuixi Road, Tianjin 300384, China

[2]Lead contact

*Correspondence: tongxinli@tju.edu.cn

https://doi.org/10.1016/j.isci.2023.107203

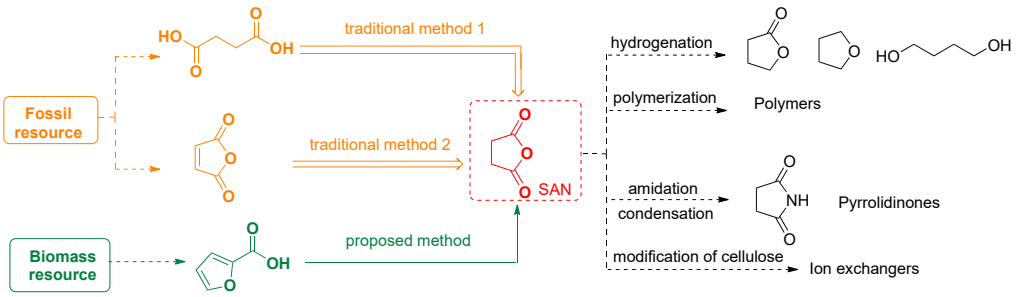

Figure 1. Production of SA from different substrates and its further application

temperature. However, by-products such as γ-butylactone and tetrahydrofuran are often generated except for obtaining SAN during the hydrogenation process.

In the different biomass-derived furanic platform compounds, furfural (FUR) is industrially produced from the cornstalks via the simple dehydration process.[33] Also, furoic acid (FAC) and furfuryl alcohol (FAL) are easily obtained from the oxidation[34–36] and hydrogenation reaction[37,38] of FUR under mild conditions. Therefore, the further transformation of FAC, FUR, and FAL to value-added chemicals can promote and enlarge the efficient utilization of renewable feedstocks. In particular, the generation of C4 chemicals from the furanic platform compounds can be used as important building blocks for the production of liquid hydrocarbon fuels or fuel additives. In the previous study, the generation of C4 dicarboxylic acids including maleic acid, fumaric acid, succinic acid, and maleic anhydride (MAN) have been achieved using the suitable catalytic systems;[39,40] however, the one-step direct preparation of SAN from the furanic platform compound is still a challenge in the chemical field.

In this article, a mild and efficient production of SAN is developed through the photocatalytic oxygenation of FAC, FUR, and FAL with *m*-tetraphenyl porphyrin (H_2TPP) in the presence of molecular oxygen (O_2). Therein, during the oxygenation process of FAC with O_2, a 99.9% conversion and a 97.8% selectivity of SAN is acquired in ethyl acetate under the visible light. Similarly, the photocatalytic oxygenation of FUR and FAL also selectively generate SAN when the reaction is performed under the suitable conditions. Moreover, the selectivity of product could be purposefully regulated and controlled by adjusting the light intensity and reaction time. Furthermore, the investigations of reaction mechanisms reveal that SAN is mainly produced via the selective transformation of the *in situ* produced intermediate 5-hydroxy-2(5H)-furanone (5-HFO) under the visible light. It provides a novel catalytic strategy for the sustainable production of SAN from biomass resources. There exist some obvious advantages, such as the excellent product yield, the mild reaction conditions, high atomic efficiency, and the low pollution to the environment. Therefore, this process is very promising in replacing traditional preparation methods of SAN in the chemical industry.

RESULTS

Catalyst screening

Initially, the catalytic activities of different metal and substituted porphyrins on photocatalytic oxygenation of FAC were evaluated with O_2 as the terminal oxidant in acetonitrile (CH_3CN) solvent at room temperature. As indicated in the Scheme 1, the obtained products are mainly SAN, 5-HFO, and a small amount of MAN, which have been identified by the GC-MS and NMR spectra. The experimental data are shown

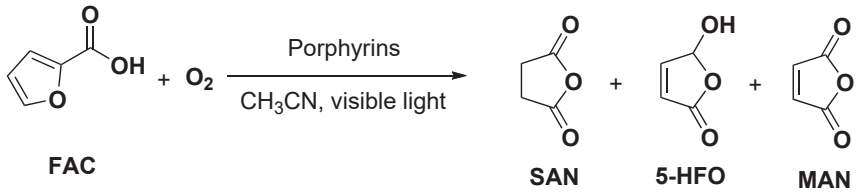

Scheme 1. Equation for the transformation of FAC under the visible light

Table 1. Selective oxygenation of FAC using different photocatalysts

Entry	Catalyst[a]	Solvent	Conv. (%)[b]	Product distribution (%)[b]		
				SAN	5-HFO	MAN + others
1	FeTClPP	CH_3CN	18.9	1.3	93.0	5.7
2	MnTClPP	CH_3CN	27.0	1.3	93.7	5.0
3	CuTPP	CH_3CN	99.0	20.4	58.4	21.2
4	ZnTPP	CH_3CN	99.0	29.0	57.2	53.3
5	H_2TPP	CH_3CN	99.0	46.0	40.5	13.5 (4.2/9.3)
6	H_2TCPP	CH_3CN	99.0	12.7	69.9	17.4
7	H_2TCNPP	CH_3CN	99.0	43.8	43.7	12.5
8	H_2TMPP	CH_3CN	99.9	33.7	49.7	16.6
9[c]	H_2TPP	CH_3CN	99.9	68.7	21.0	10.3
10	none	CH_3CN	26.5	3.8	89.4	6.8
11[c]	H_2TPP	Acetone	99.9	89.3	9.7	2.8
12[c]	H_2TPP	Ethyl acetate	99.9	97.8	2.0	0.2
13[c]	H_2TPP	DMF	99.0	7.2	32.1	60.7
14[c]	H_2TPP	DMSO	99.0	–	–	>99.9
15[c]	H_2TPP	Toluene	99.0	16.8	57.6	25.6
16	H_2TPP	n-hexane	99.0	45.0	25.3	29.7
17	H_2TPP	octane	99.0	12.9	49.4	37.7

[a]Reaction conditions: 0.1g of FAC, 0.001g of catalyst, and 10 mL of solvent was added to reactor, and the oxidation was performed at 0.3 MPa of O_2 under 300 mw Xe lamp for 10 h.
[b]The data are obtained by GC analysis with the internal standard method.
[c]The reaction was carried out using 400 mw Xe lamp.

in Table 1. When the tetra (*p*-chloro phenyl) porphyrin iron (FeTClPP) or tetra (*p*-chlorophenyl) porphyrin manganese (MnTClPP) is employed as the photocatalyst, the oxidation reaction occurs where the conversion is, respectively, 18.9% or 27.4%, and 5-HFO is the main product under visible light. Then, about 99% conversion was obtained in the presence of tetraphenylporphyrin copper (CuTPP) or tetraphenylporphyrin zinc (ZnTPP) photocatalyst, where the selectivity of SAN was 20.4% or 29%, respectively. In addition, the catalytic performances of the metal-free porphyrins were investigated, and it is found that all the conversions of FAC arrived at 99% when tetra (4-carboxylphenyl) porphyrin (H_2TPP), tetra (4-carboxylphenyl) porphyrin (H_2TCPP), tetra (*p*-methylphenyl) porphyrin (H_2TMPP), and tetra (*p*-cyanophenyl) porphyrin (H_2TCNPP) were used as photocatalysts in the oxidation reaction; however, the selectivity of product was quite different, in which the selectivity of SAN can reach about 46.0% with H_2TPP as the catalyst. Furthermore, the conversion and the selectivity of SAN respectively increased to 99.9% and 68.7% if the oxygenation of FAC was performed under a 400 mW Xe lamp. Next, to verify the promotion action of photocatalysts, the blank experiment was carried out under the same conditions. As a result, only 26.5% conversion and 3.8% selectivity of SAN was attained in the absence of any catalyst. Considering the high selectivity of SAN and its good catalytic activity, H_2TPP was selected as the photocatalyst for further investigations and optimization during the FAC oxidation process.

Next, the influence of the reaction medium on the photocatalytic oxygenation of FAC was studied under 400 mW Xe lamp. The experimental results exhibited that the use of acetone and ethyl acetate as the solvents could improve the production of SAN; especially, the conversion of FAC and the selectivity of SAN arrived at 99% and 97.8% in ethyl acetate, respectively. However, using the toluene, DMF or DMSO as the solvent, the SAN was not the main product during the reaction. In the DMF solvent, both the SAN and 5-HFO were generated a little under similar conditions. Moreover, neither SAN nor 5-HFO was detected in the DMSO solvent, which keeps consistent with the removal performance of DMSO to $^1O_2$ during reaction. With toluene as the solvent, only 16.8% selectivity of SAN was acquired, where 5-HFO was majorly achieved and the selectivity was about 57.6%. Furthermore, *ca.* 45% and 12.9% selectivity of SAN was attained when n-hexane and octane was used as solvent. These indicate that the solvent plays a crucial

Table 2. The photocatalytic oxygenation of FAC under different conditions

Entry	Light supply[a]	Time (h)	Conv. (%)[b]	Product distribution (%)[b]			
				SAN	5-HFO	MAN	others
1	no light	10	–	–	–	–	–
2[c]	Xe lamp, 400 mW	10	2.6	–	–	–	–
3	Xe lamp, 210 mW	10	99.9	4.3	80.0	0.4	15.3
4	Xe lamp, 250 mW	10	99.9	5.8	79.0	0.5	14.7
5	Xe lamp, 300 mW	10	99.9	35.7	54.5	0.4	9.4
6	Xe lamp, 350 mW	10	99.9	59.6	34.1	0.4	5.9
7	Xe lamp, 500 mW	8	99.9	97.3	2.2	0.5	–
8	Xe lamp, 210 mW	30	99.9	97.1	2.4	0.5	–
9	Solar simulator	10	84.5	1.6	80.7	0.3	17.4
10	Solar simulator	40	99.9	74.8	20.7	0.4	4.1

[a]Reaction conditions: 0.1 g of FAC, 0.001 g of H_2TPP and 10 mL ethyl acetate is added to reactor, under 0.3 MPa of O_2, at a certain light intensity.
[b]The data are obtained by the GC analysis with the internal standard method.
[c]The reaction was performed in the absence of molecular oxygen.

role on the selective preparation of SAN under the visible light. From the obtained results, it can be concluded that ethyl acetate as solvent is the most effective for SAN production in the photocatalytic oxygenation of FAC with O_2 as oxidant.

The effects of light intensity and reaction time

Table 2 gives the results of FAC oxidation in ethyl acetate under different light irradiation. Therein, no reaction happens under no visible light or in the absence of O_2 (entries 1 and 2), indicating that the light and the O_2 are essential for the direct photocatalytic oxygenation of FAC to SAN. Moreover, when the light intensity of Xe lamp is decreased to 210 mw, only 4.3% selectivity of SAN was obtained, whereas the selectivity of 5-HFO arrived at 80% (entry 3). Furthermore, the photocatalytic oxygenation of FAC were tested at 250 mW, 300 mW, and 350 mW of light intensity, respectively (entries 4 to 6); as a result, it is found that the selectivity of SAN is gradually elevated while the selectivity of 5-HFO was slowly decreased when the light intensity was raised from 210 mW to 350 mW. Especially, a 99.9% conversion with 97.3% yield of SAN can be obtained when the oxidation is carried out at the light intensity of 500 mW for 8 h in an ambient temperature. Thus, it is concluded that the amount of light intensity is closely related to the selectivity of product, and the high light intensity is helpful to the generation of SAN in photocatalytic FAC oxygenation. On the other hand, if the reaction time is extended to 30 h at a light intensity of 210 mW, the SAN selectivity can reach 97.1%; meanwhile, the selectivity of 5-HFO is declined to 2.4% with the extending of time (entry 7). These results exhibited that 5-HFO should be first produced during the photocatalytic oxygenation of FAC, and is further isomerized to generate the SAN in this reaction system. Also, at the high light intensity, the isomerization of 5-HFO to the SAN is greatly accelerated. In the following, the solar simulator was further used as light supply in the oxygenation process of FAC, where 5-HFO is the main product at the beginning stage, and about 84.5% conversion with 80.7% selectivity of 5-HFO was attained for 10 h (entry 9). With the prolonging of the reaction time, the amount of the generated SAN was gradually increased, and a 99.9% FAC conversion in a 74.8% selectivity of SAN as the main product was obtained after 40 h (entry 10). It is known that the solar simulator as light source is near natural light; accordingly, this photocatalytic process is very promising to the industrial production of SAN under ambient conditions.

Subsequently, the effect of time on the FAC conversion and the selectivity of SAN was investigated at the light intensity of 210 mW and 400 mW, respectively, and the results are shown in the Figure 2. When the used light intensity was 210 mW, the conversion of FAC gradually rose as the time increased from 10 min to 40 min. A 99% conversion of FAC in 80.7% selectivity of 5-HFO was obtained after 40 min, and then the FAC conversion and the product distribution remained almost unchanged when the time was prolonged to 1 h or longer. Combined with the above result of entry 3 of Table 2, it can be concluded that the formed product is majorly 5-HFO, and only a small amount of SAN is produced before 10 h in the reaction

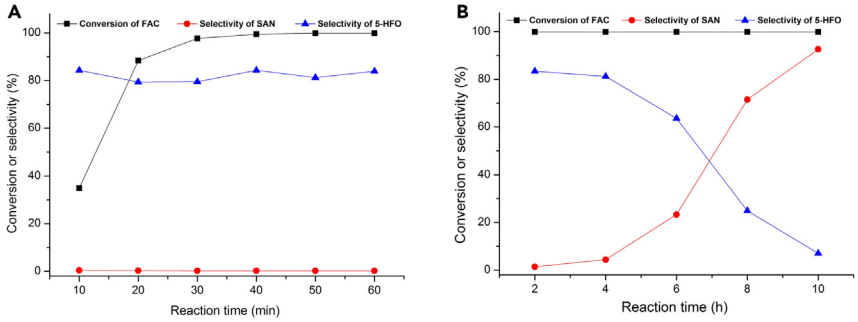

Figure 2. The influence of time on photocatalytic transformation of FAC under the visible light

(A) With the light intensity of 210 mW.

(B) With the light intensity of 400 mW).

with a light intensity of 210 mw. However, when light intensity was enhanced to 400 mW, the selectivity of SAN increased gradually, and the 5-HFO selectivity declined with the time being extended from 2 h to 10 h, in which all the conversions of FAC arrived at 99.9% in these photocatalytic oxygenation processes. Notably, a 97.8% selectivity of SAN was obtained after 10 h. These results verified the oxygenation of FAC is a tandem reaction, and 5-HFO is a key intermediate during the production of SAN via the photocatalytic selective conversion of FAC under the visible light.

Photocatalytic oxygenation of FUR and FAL with H_2TPP under the visible light

To enlarge the scope of the reactant, the transformation of FUR and FAL were also studied with H2TPP under the visible light, and the obtained data are presented in Tables 3 and 4, respectively. In the photocatalytic transformation of FUR, the use of solvent is closely related to the selectivity of the product; in CH_3CN, acetone, and ethyl acetate, the main formed product is MAN where the selectivity of SAN is, respectively, 13.5%, 23.3%, and 32.8%, indicating that ethyl acetate as solvent is still the most advantageous to the production of SAN under the visible light. Moreover, when the light intensity declined to 210 mW, only 18.7% selectivity of SAN was obtained which is consistent with that in the photocatalytic FAC transformation. However, using DMF, toluene, and 1,4-dioxane as solvents, very little SAN and MAN were generated.

Table 3. Selective oxygenation of FUR with the H_2TPP under the visible light

				Product distribution (%)[b]			
Entry	Solvent[a]	Additive	Conv. (%)[b]	SAN	5-HFO	MAN	Others
1	CH_3CN	–	>99.9	13.5	11.5	63.0	12.0
2	Acetone	–	98.4	23.3	4.3	58.4	14.1
3	Ethyl acetate	–	95.7	32.8	–	60.1	7.1
4[c]	Ethyl acetate	–	74.0	18.7	5.7	65.8	9.7
5	DMF	–	99.2	3.0	1.5	18.5	77.0
6	Toluene	–	87.1	6.4	–	3.7	89.9
7	1,4-dioxane	–	99.7	16.1	2.0	10.5	71.4
8	CH_3CN	HOAc	>99.9	19.5	13.7	53.8	13.0
9	Ethyl acetate	benzoic acid	95.6	40.0	–	50.3	9.7
10	Ethyl acetate	HCl	96.1	52.3	–	31.9	15.8
11	Ethyl acetate	H_2O_2	94.2	55.9	–	38.5	5.6
12[d]	Ethyl acetate	H_2O_2	90.9	17.1	30.3	–	30.8

[a]Reaction conditions: 0.1 g of FUR, 0.001 g of H_2TPP, and 10 mL of solvent was added to reactor, under 0.3 MPa of O_2 at the light intensity of 300 mW Xe lamp, for 10 h.

[b]The data are obtained by GC analysis with the internal standard method.

[c]The reaction was carried out with a light intensity of 210 mW Xe lamp.

[d]In a nitrogen atmosphere.

Table 4. Selective oxygenation of FAL with the H_2TPP under the visible light

Entry	Light intensity[a]	Additive	Conv. (%)[b]	Product distribution (%)[b]			
				SAN	5-HFO	MAN	Others
1	210 mW	–	>99.9	64.7	21.7	13.6	–
2	400 mW	–	>99.9	89.9	–	10.1	–
3	400 mW	benzaldehyde	>99.0	82.6	–	14.6	2.7[c]
4	400 mW	benzoic acid	>99.9	91.7	–	8.3	–

[a]Reaction: 0.1g of FAL, 0.001g of H_2TPP, in 10 mL ethyl acetate, at a 0.3 MPa of O_2, under the light irradiation of Xe lamp, for 10 h.
[b]The results are obtained by GC with the internal standard technique.
[c]The by-product is FUR except 5-HFO and MAN during the reaction.

Next, the effect of different additives was investigated; as a result, the addition of organic acid HOAc and benzoic acid is helpful to improve SAN selectivity in either CH_3CN solvent or ethyl acetate, which proves that the existence of H^+ can promote the formation of SAN to some extent. Also, it is found that the promotion of HCl and hydrogen peroxide in the production of SAN is more obvious, and 52.3% and 55.9% selectivity of SAN could be acquired in the ethyl acetate system. Therein, the selectivity 5-HFO increases a lot while MAN is not detected when hydrogen peroxide is added to reaction in a nitrogen atmosphere. The above results demonstrate that the selectivity of product in the FUR transformation is controllable by tuning the photocatalytic reaction conditions.

For the photocatalytic oxygenation of FAL with H_2TPP under the visible light, the main formed product is also the SAN in ethyl acetate solvent, in which the selectivity of SAN is 64.7% and 89.9% under the light intensity of 210 mW and 400 mW, respectively. In addition, the influence of the aldehyde and organic acid was also determined; as a result, it was found that addition of benzaldehyde was beneficial to the formation of MAN whereas the participation of benzoic acid was helpful in enhancing the selectivity of SAN in the reaction. These data exhibited the action of the aldehyde group and carboxyl group and further confirmed the results of the photocatalytic oxygenation of FAC and FUR with H_2TPP under visible light. Based on the above investigations, it can be seen that both FUR and FAL can also be employed to efficiently produce SAN by choosing the suitable conditions.

The study on the active oxygen species in reactions

To study the photocatalytic reaction mechanism, a series of control experiments have been performed to test the active oxygen species during reactions. As indicated in Table 5, no reaction occurs when beta carotene is added as the inhibitor of singlet oxygen ($^1O_2$), providing powerful evidence that $^1O_2$ is a significant

Table 5. The results of control experiments for studying reaction mechanisms[a]

Entry[a]	Scavenger or additive	Conv. (%)[b]	Product distribution (%)[b]			
			SAN	5-HFO	MAN	Others
1	no	>99.9	0.2	83.9	0.1	15.7
2	beta carotene	0	–	–	–	–
3	p- benzoquinone	99.7	0.3	79.0	1.5	19.2
4	t-butanol	>99.9	0.5	79.3	0.5	19.7
5	TEMPO	>99.9	0.5	82.1	2.0	15.4
6[c]	benzaldehyde	>99.9	84.1	–	5.7	10.2
7[d]	benzaldehyde	>99.9	35.2	38.0	12.1	14.7

[a]Reaction conditions: 0.1 g FAC, 0.001 g H_2TPP, 0.1 g additive, in 10 mL ethyl acetate solvent, under 0.3 MPa of O_2, at the light intensity of 210 mW with Xe lamp, reaction time 1 h.
[b]The data were obtained by GC with the internal standard method.
[c]The reaction was carried out at the light intensity of 400 mW.
[d]The reaction was performed with 0.001 g H_2TPP in CH_3CN solvent at a light intensity 300 mW for 10 h.

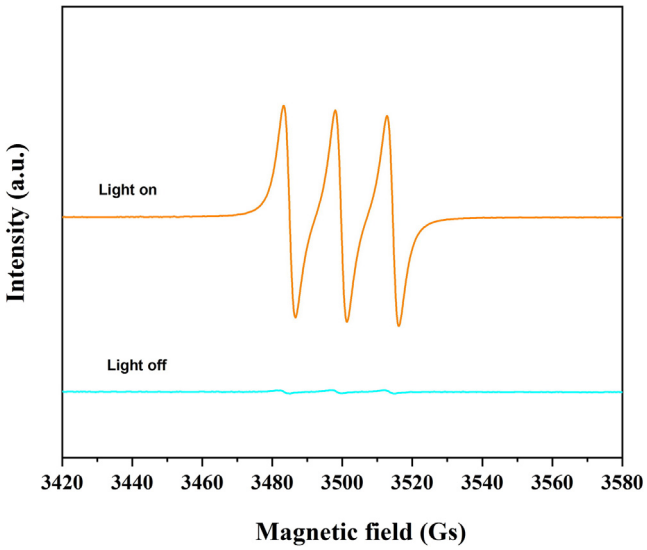

Figure 3. The EPR results for the capture of active oxygen species

active species during the FAC transformation. However, the conversion and product selectivity remain basically unchanged when *p*-benzoquinone or t-butanol is employed as the scavenger of $O_2^{\cdot-}$ or ·OH, indicating that the $O_2^{\cdot-}$ or ·OH is not the main oxygen species in the reaction system. Next, to further reveal the effect of carbon-free radicals on the photocatalytic oxygenation process, a certain amount of 2, 2, 6, 6-tetramethyl-1-piperinedinyloxy (TEMPO) was added to the system; as a result, the conversion and product selectivity also remained almost unchanged, which indicates that the amount of carbon-free radicals was very rare during the transformation of FAC with H_2TPP under the visible light. On the other hand, if benzaldehyde was added, there was no 5-HFO being detected after the reaction, where the selectivity of SAN decreased to 84.1%, and the selectivity of MAN increased to 5.7%; it showed that the existence of the aldehyde group can promote the generation of MAN from the conversion of 5-HFO and drop the isomerization of 5-HFO to produce SAN under the visible light.

To further verify the existence of the $^1O_2$ active species, EPR detection was also performed, in which 2, 2, 6, 6-tetramethylpiperidone (TEMP) was employed to capture the $^1O_2$ generated during the photocatalytic oxygenation process of FAC with H_2TPP under the visible light. The obtained data are presented in the Figure 3. It can be seen that there was no signal in the absence of light, and triple peaks of equal intensity, e.g., the characteristic signal peak of $^1O_2$ were observed under the visible light. These adequately prove that $^1O_2$ active species was generated in the reaction, which is in agreement with the control experiment results.

DISCUSSION

The performance of different catalysts

The metal and substituted porphyrins as photocatalysts exhibited different activities on the direct production of SAN from the transformation of FAC with O_2 under the visible light. To explore the relationship between the physiochemical property and catalytic activity, the UV-vis spectra of the used catalysts were determined and the data are shown in Figure 4. It can be seen that the main adsorption of different porphyrin-based photocatalysts locates 375 nm–440 nm, where the adsorption abilities of the H_2TPP and ZnTPP are much higher than those of other catalysts. This should be responsible for their excellent performances during the reaction. In addition, when the molecular H_2TPP contains either electron-donating groups or electron-withdrawn groups, the conversion of FAC is slightly improved whereas the selectivity of SAN declines to some extent, which can be attributed to a combination of electron effect and steric effect during the photocatalytic processes.

The effects of light intensity and time on the product distribution

Based on the experimental data of the above Table 2 and Figure 2, the product distribution in the photocatalytic oxygenation of FAC with O_2 can be regulated by changing the conditions. Therein, high light

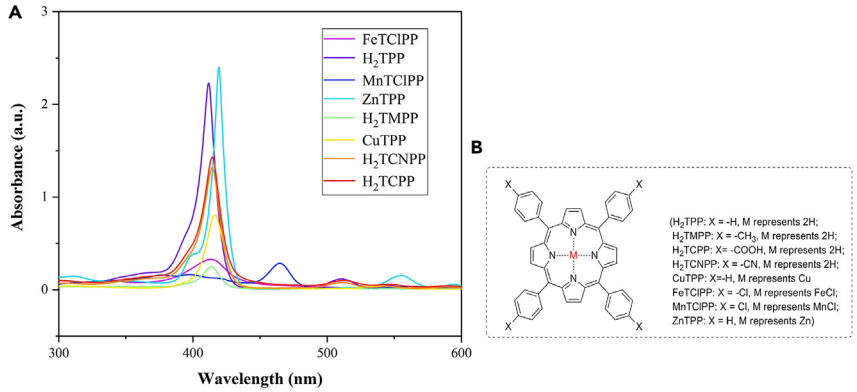

Figure 4. The UV-vis spectra (A) and the structures (B) of different porphyrin-based photocatalysts

intensity (400 mW) facilitates the formation of target product SAN; whereas, the selectivity of 5-HFO often reaches very high (>80%) at a relatively low light intensity (210 mW). This should be due to the fact that the isomerization process of 5-HFO to SAN is more rapid at high light intensity. Moreover, product distribution is closely related to the reaction time. As seen from the results of Figure 2B, the photocatalytic oxygenation is a tandem reaction process. With the prolonging of time, the selectivity of SAN increased gradually and the 5-HFO selectivity declined, where the above 81% selectivity of 5-HFO with a 99.9% conversion of FAC was obtained after 2 h, and the selectivity of SAN arrived at 97.8% when the reaction was further performed for 10 h. Thus, the main product should be controllable in photocatalytic oxygenation of FAC with H_2TPP under the visible light. 5-HFO can also be selectively obtained by tuning the light intensity and reaction time, except for the efficiently producing SAN with FAC as reactant. Notably, at a light intensity of 210 mW, the selectivity of 5-HFO can remain a high value during the reaction time of 40 min to 10 h, which provides a way to prepare 5-HFO as the value-added chemical product.

The functions of -CHO and -COOH groups

Compared to the reaction of FAC and FUR under similar conditions, it is found that the molecular structure (-CHO group and -COOH group) of substrates was closely related to the product distribution in the photocatalytic oxygenation processes. As a result, the existence of -COOH tends to generate the target product SAN, whereas the inclusion of -CHO is beneficial in attaining MAN in the "H2TPP-O_2-visible light" reaction system. This conclusion is further proved by adding benzaldehyde or benzoic acid into the reaction (entry 9 of Table 3, and entry 7 of Table 5). Moreover, a similar phenomenon is discovered during the photocatalytic oxygenation of FAL with "H2TPP-O_2-visible light" system (entries 3 and 4 of Table 4). Herein, the promotion of -CHO to generate MAN from 5-HFO can be explained by the formation of hydroperoxides from the reaction of the aldehyde with active oxygen species, where the 5-HFO is easily converted to MAN by hydroperoxide in the reaction. The acceleration effect of -COOH could be because the proton may catalyze the isomerization process of the 5-HFO to produce SAN during the reaction (shown in Scheme 2). Also, the promotion of H^+ was further verified by the effect of acetic acid and hydrochloric acid on the FUR transformation under the visible light (entries 8 and 10 of Table 3).

Isotope labeling of reaction pathway and photocatalytic reaction mechanism

To clarify the reaction pathway between molecular oxygen and substrate, isotope labeling experiments of ^{18}O were performed. In the photocatalytic oxygenation process of FAC, the $^{18}O_2$ was used to replace the

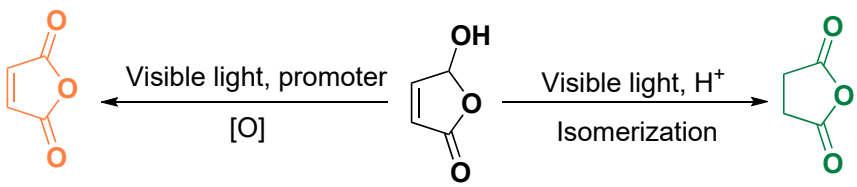

Scheme 2. The transformation routes of 5-HFO in the H_2TPP-O_2-visible light system

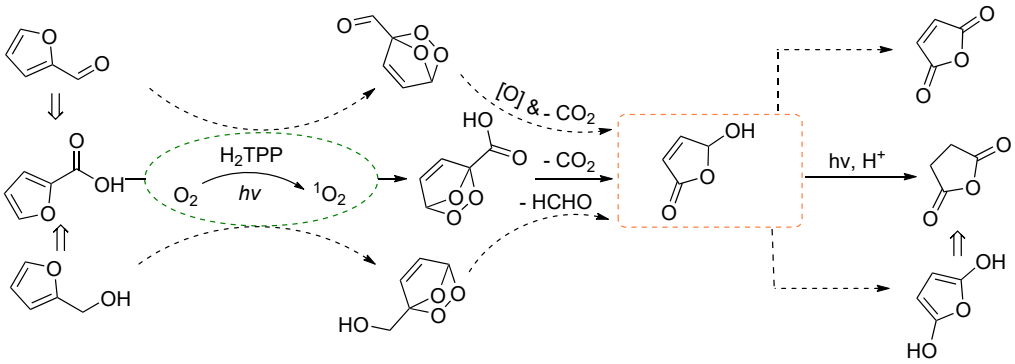

Scheme 3. Proposed mechanism for production of SAN with O_2 under the visible light

common $^{16}O_2$ as oxidant; it was found that the resulting product SAN molecule contained two ^{18}O atoms (the GC-MS spectrum is provided in supporting information). Similarly, during the photocatalytic oxygenation of FUR and FAL with $^{18}O_2$, both the SAN and MAN contained two ^{18}O atoms (GC-MS spectra are indicated in supporting information). These data indicate that the addition of singlet oxygen and furan ring introduce two O atoms into the final products, whereas the O atom in the side chain of the furans leaves to generate the high valuable C4 product with the cleavage of C-C bond during the whole reaction.

Based on the fundamental catalytic theory and the experimental results, a possible reaction mechanism for the production of SAN is proposed and shown in the Scheme 3. Therein, the O_2 is first activated to $^1O_2$ in the presence of H_2TPP photocatalyst; next, the cycloaddition reaction of FAC with $^1O_2$ occurs and the endoperoxide as intermediate I is generated. Further, intermediate I is transformed to 5-HFO through the decarboxylation and the ring-opening cleavage of -*O*-O- bond under the visible light. Finally, the 5-HFO as intermediate II can be isomerized to produce the SAN with the assistance of H^+ and high intensity light. It needs to be mentioned that another competitive route is the conversion of 5-HFO to generate the by-product MAN in the presence of O_2.

Conclusion

In summary, a photocatalytic oxygenation of biomass-derived furanic platform compounds to the value-added SAN was achieved by using metal-free H_2TPP photocatalyst in the presence of O_2. Under the optimized conditions, a 99.9% conversion with a 97.8% selectivity of SAN was obtained in the selective transformation of FAC; therein, the generation of $^1O_2$ plays a significant role and 5-HFO is confirmed to be a key intermediate. To be noted, product selectivity could be regulated by changing the light intensity and reaction time. Moreover, photocatalytic oxygenation processes of FUR and FAL to produce SAN were also successfully performed where the yield of SAN was lower than that from the reaction of FAC under the visible light. In particular, in the transformation of FUR, the generation of MAN was a competitive process. Furthermore, based on the results of EPR detection, the isotope labeling and control experiments, a possible reaction mechanism is proposed. It provides an efficient approach to directly synthesize the high valuable C4 products from biomass-based furanic platform compounds in the chemical industry.

Limitations of the study

In this study, the production of C4 chemicals from substituted furans (C5) requires the cleavage of C-C bond on the side chain of the furan cycle. The substituted group (-COOH, CHO, CH_2OH) should be closely associated with the photocatalytic reaction process. Thus, the limitation of the present work is the influence of the group on the side chain to the SAN production. The C-C bond cleavage and the effect of substituent groups can be explored utilizing theoretical calculation and *in situ* spectroscopy techniques in future studies.

STAR★METHODS

Detailed methods are provided in the online version of this paper and include the following:

- KEY RESOURCES TABLE
- RESOURCE AVAILABILITY

SUPPLEMENTAL INFORMATION

Supplemental information can be found online at https://doi.org/10.1016/j.isci.2023.107203.

ACKNOWLEDGMENTS

This research work was financially supported by the National Natural Science Foundation of China (21878235).

AUTHOR CONTRIBUTIONS

X.G. conducted the valuation experiments; X.T. designed the experiments and wrote the paper; Y.Z. detected the structure of product; S.X. analyzed the characterization results.

DECLARATION OF INTERESTS

The authors declare no competing interests.

INCLUSION AND DIVERSITY

We support inclusive, diverse, and equitable conduct of research.

Received: March 16, 2023
Revised: April 11, 2023
Accepted: June 21, 2023
Published: June 25, 2023

REFERENCES

1. Deng, F., and Amarasekara, A.S. (2021). Catalytic upgrading of biomass derived furans. Ind. Crops Prod. *159*, 113055. https://doi.org/10.1016/j.indcrop.2020.113055.

2. Natsir, T.A., and Shimazu, S. (2020). Fuels and fuel additives from furfural derivatives via etherification and formation of methylfurans. Fuel Proc. Technol. *200*, 106308. https://doi.org/10.1016/j.fuproc.2019.106308.

3. Zhao, Y., Lu, K., Xu, H., Zhu, L., and Wang, S. (2021). A critical review of recent advances in the production of furfural and 5-hydroxymethylfurfural from lignocellulosic biomass through homogeneous catalytic hydrothermal conversion. Renew. Sustain. Energy Rev. *139*, 110706. https://doi.org/10.1016/j.rser.2021.110706.

4. Jing, Y., Guo, Y., Xia, Q., Liu, X., and Wang, Y. (2019). Catalytic production of value-added chemicals and liquid fuels from lignocellulosic biomass. Chem *5*, 2520–2546. https://doi.org/10.1016/j.chempr.2019.05.022.

5. Nakagawa, Y., Tamura, M., and Tomishige, K. (2013). Catalytic reduction of biomass-derived furanic compounds with hydrogen. ACS Catal. *3*, 2655–2668. https://doi.org/10.1021/cs400616p.

6. Liu, X., Li, B., Han, G., Liu, X., Cao, Z., Jiang, D.E., and Sun, Y. (2021). Electrocatalytic synthesis of heterocycles from biomass-derived furfuryl alcohols. Nat. Commun. *12*, 1868. https://doi.org/10.1038/s41467-021-22157-5.

7. Hermens, J.G.H., Jensma, A., and Feringa, B.L. (2022). Highly efficient biobased synthesis of acrylic acid. Angew. Chem. Int. Ed. Engl. *61*, e202112618. https://doi.org/10.1002/ange.202112618.

8. Shen, G., Andrioletti, B., and Queneau, Y. (2020). Furfural and 5-(hydroxymethyl)furfural: two pivotal intermediates for bio-based chemistry. Curr. Opin. Green Sustain. Chem. *26*, 100384. https://doi.org/10.1016/j.cogsc.2020.100384.

9. Küksal, A., Klemm, E., and Emig, G. (2002). Reaction kinetics of the liquid-phase hydrogenation of succinic anhydride on CuZnO-catalysts with varying copper-to-zinc ratios in a three-phase slurry reactor. Appl. Catal. A: General. *228*, 237–251. https://doi.org/10.1016/S0926-860X(01)00978-4.

10. Budroni, G., and Corma, A. (2008). Gold and gold - platinum as active and selective catalyst for biomass conversion: synthesis of γ-butyrolactone and one-pot synthesis of pyrrolidone. J. Catal. *257*, 403–408. https://doi.org/10.1016/j.jcat.2008.05.031.

11. Liu, Y., Fu, J., Ren, D., Song, Z., Jin, F., and Huo, Z. (2018). Efficient synthesis of succinimide from succinic anhydride in water over unsupported nanoporous nickel material. ChemistrySelect *3*, 724–728. https://doi.org/10.1002/slct.201703154.

12. Cushman, M., and Castagnoli, N., Jr. (1971). Condensation of succinic anhydrides with Schiff bases Scope and mechanism. J. Org. Chem. *36*, 3404–3411. https://doi.org/10.1021/jo00821a029.

13. Maeda, Y., Nakayama, A., Kawasaki, N., Hayashi, K., Aiba, S., and Yamamoto, N. (1997). Ring-opening copolymerization of succinic anhydride with ethylene oxide initiated by magnesium diethoxide. Polymer *38*, 4719–4725. https://doi.org/10.1016/S0032-3861(96)01088-9.

14. Girek, T., Kozlowski, C., Koziol, J., Walkowiak, W., and Korus, I. (2005). Polymerisation of β-cyclodextrin with succinic anhydride.

Synthesis, characterisation, and ion flotation of transition metals. Carbohydr. Polym. *59*, 211–215. https://doi.org/10.1016/j.carbpol.2004.09.011.

15. Yashiro, T., Kricheldorf, H.R., and Huijser, S. (2009). Syntheses of polyesters from succinic anhydride and various diols catalyzed by metal triflates. Macromol. Chem. Phys. *210*, 1607–1616. https://doi.org/10.1002/macp.200900189.

16. Li, W., Jin, A., Liu, C., Sun, R., Zhang, A., and Kennedy, J.F. (2009). Homogeneous modification of cellulose with succinic anhydride in ionic liquid using 4-dimethylaminopyridine as a catalyst. Carbohydr. Polym. *78*, 389–395. https://doi.org/10.1016/j.carbpol.2009.04.028.

17. Melo, J.C., Silva Filho, E.C., Santana, S.A., and Airoldi, C. (2011). Synthesized cellulose/succinic anhydride as an ion exchanger. Calorimetry of divalent cations in aqueous suspension. Thermochim. Acta *524*, 29–34. https://doi.org/10.1016/j.tca.2011.06.007.

18. Davidson, D., and Newman, P. (1952). The occurrence of anhydrides in the pyrolysis of monocarboxylic acids. J. Am. Chem. Soc. *74*, 1515–1516. https://doi.org/10.1021/ja01126a048.

19. Chen, Y., Wang, Z., Liu, S., and Zhang, G. (2022). Modified niobic acid via acidification by various liquid acids for dehydration of succinic acid to succinic anhydride. Colloids. Surf. A: Physicochem. Eng. Asp. *650*, 129644. https://doi.org/10.1016/j.colsurfa.2022.129644.

20. Pillai, U.R., Sahle-Demessie, E., and Young, D. (2003). Maleic anhydride hydrogenation over Pd/Al_2O_3 catalyst under supercritical CO_2 medium. Appl. Catal. B Environ. *43*, 131–138. https://doi.org/10.1016/S0926-3373(02)00305-3.

21. Wang, J., Sun, C., Xia, W., Cao, Z., Sheng, G., and Xie, X. (2022). Pd/BN catalysts for highly efficient hydrogenation of maleic anhydride to succinic anhydride. Appl. Catal. A: General. *630*, 118471. https://doi.org/10.1016/j.apcata.2021.118471.

22. Li, J., Tian, W.P., and Shi, L. (2010). Hydrogenation of maleic anhydride to succinic anhydride over $Ni/HY\text{-}Al_2O_3$. Ind. Eng. Chem. Res. *49*, 11837–11840. https://doi.org/10.1021/ie101072v.

23. Feng, Y., Yin, H., Wang, A., Xie, T., and Jiang, T. (2012). Selective hydrogenation of maleic anhydride to succinic anhydride catalyzed by metallic nickel catalysts. Appl. Catal. A: General. *425–426*, 205–212. https://doi.org/10.1016/j.apcata.2012.03.023.

24. Guo, S., and Shi, L. (2013). Synthesis of succinic anhydride from maleic anhydride on Ni/diatomite catalysts. Catal. Today *212*, 137–141. https://doi.org/10.1016/j.cattod.2012.10.004.

25. Huo, W., Zhang, C., Yuan, H., Jia, M., Ning, C., Tang, Y., Zhang, Y., Luo, J., Wang, Z., and Zhang, W. (2014). Vapor-phase selective hydrogenation of maleic anhydride to succinic anhydride over Ni/TiO_2 catalysts. J. Ind. Eng. Chem. *20*, 4140–4145. https://doi.org/10.1016/j.jiec.2014.01.012.

26. Liao, X., Zhang, Y., Hill, M., Xia, X., Zhao, Y., and Jiang, Z. (2014). Highly efficient Ni/CeO_2 catalyst for the liquid phase hydrogenation of maleic anhydride. Appl. Catal. A: General. *488*, 256–264. https://doi.org/10.1016/j.apcata.2014.09.042.

27. Torres, C.C., Alderete, J.B., Mella, C., and Pawelec, B. (2016). Maleic anhydride hydrogenation to succinic anhydride over mesoporous Ni/TiO_2 catalysts: Effects of Ni loading and temperature. J. Mol. Catal. Chem. *423*, 441–448. https://doi.org/10.1016/j.molcata.2016.07.037.

28. Tan, J., Xia, X., Cui, J., Yan, W., Jiang, Z., and Zhao, Y. (2019). Efficient tuning of surface nickel species of the Ni-phyllosilicate catalyst for the hydrogenation of maleic anhydride. J. Phys. Chem. C *123*, 9779–9787. https://doi.org/10.1021/acs.jpcc.8b11972.

29. Cai, J., Zhu, J., Zuo, L., Fu, Y., and Shen, J. (2018). Effect of surface acidity/basicity on the selective hydrogenation of maleic anhydride to succinic anhydride over supported nickel catalysts. Catal. Commun. *110*, 93–96. https://doi.org/10.1016/j.catcom.2018.02.016.

30. Li, Y.J., Qi, T.T., Dong, Y.N., Hou, W.H., Chu, G.W., Zhang, L.L., and Sun, B.C. (2022). Synthesized Ni/MMO catalysts via ultrathin Ni-Al-LDH in a rotating packed bed for hydrogenation of maleic anhydride. Fuel *326*, 125035. https://doi.org/10.1016/j.fuel.2022.125035.

31. Meyer, C.I., Marchi, A.J., Monzon, A., and Garetto, T.F. (2009). Deactivation and regeneration of Cu/SiO_2 catalyst in the hydrogenation of maleic anhydride. Kinetic modeling. Appl. Catal. A Gen. *367*, 122–129. https://doi.org/10.1016/j.apcata.2009.07.041.

32. Li, J., Tian, W.P., Wang, X., and Shi, L. (2011). Nickel and nickel–platinum as active and selective catalyst for the maleic anhydride hydrogenation to succinic anhydride. Chem. Eng. J. *175*, 417–422. https://doi.org/10.1016/j.cej.2011.09.023.

33. Mamman, A.S., Lee, J.-M., Kim, Y.-C., Hwang, I.T., Park, N.-J., Hwang, Y.K., Chang, J.-S., and Hwang, J.-S. (2008). Furfural: hemicellulose/xylose-derived biochemical. Biofuel. Bioprod. Biorefin. *2*, 438–454. https://doi.org/10.1002/bbb.95.

34. Hurd, C.D., Garrett, J.W., and Osborne, E.N. (1933). Furan Reactions. IV. Furoic acid from furfural. J. Am. Chem. Soc. *55*, 1082–1084. https://doi.org/10.1021/ja01330a032.

35. Verdeguer, P., Merat, N., Rigal, L., and Gaset, A. (1994). Optimization of experimental conditions for the catalytic oxidation of furfural to furoic acid. J. Chem. Technol. Biotechnol. *61*, 97–102. https://doi.org/10.1002/jctb.280610203.

36. Nocito, F., Ditaranto, N., Linsalata, D., Naschetti, M., Comparelli, R., Aresta, M., and Dibenedetto, A. (2022). Selective aerobic oxidation of furfural into furoic acid over a highly recyclable $MnO_2@CeO_2$ core - shell oxide: the role of the morphology of the catalyst. ACS Sustain. Chem. Eng. *10*, 8615–8623. https://doi.org/10.1021/acssuschemeng.2c02341.

37. Villaverde, M.M., Bertero, N.M., Garetto, T.F., and Marchi, A.J. (2013). Selective liquid-phase hydrogenation of furfural to furfuryl alcohol over Cu-based catalyst. Catal. Today *213*, 87–92. https://doi.org/10.1016/j.cattod.2013.02.031.

38. Jiménez-Gómez, C.P., Cecilia, J.A., Durán-Martín, D., Moreno-Tost, R., Santamaría-González, J., Mérida-Robles, J., Mariscal, R., and Maireles-Torres, P. (2016). Gas-phase hydrogenation of furfural to furfuryl alcohol over Cu/ZnO catalysts. J. Catal. *336*, 107–115. https://doi.org/10.1016/j.jcat.2016.01.012.

39. Zhu, J., and Yin, G. (2021). Catalytic transformation of the furfural platform into bifunctionalized monomers for polymer synthesis. ACS Catal. *11*, 10058–10083. https://doi.org/10.1021/acscatal.1c01989.

40. Mariscal, R., Maireles-Torres, P., Ojeda, M., Sádaba, I., and López Granados, M. (2016). Furfural: a renewable and versatile platform molecule for the synthesis of chemicals and fuels. Energy Environ. Sci. *9*, 1144–1189. https://doi.org/10.1039/C5EE02666K.

STAR★METHODS

KEY RESOURCES TABLE

REAGENT or RESOURCE	SOURCE	IDENTIFIER
Chemicals, peptides, and recombinant proteins		
Acetonitrile (CH_3CN)	Aladdin Co.,Ltd.	CAS:75-05-8
Toluene	Aladdin Co. Ltd.	CAS:108-88-3
n-Hexane	Aladdin Co. Ltd.	CAS:110-54-3
Octane	Aladdin Co. Ltd.	CAS:111-65-9
Furoic acid (FAC)	Aladdin Co. Ltd.	CAS:88-14-2
Furfuryl alcohol (FAL)	Aladdin Co. Ltd.	CAS:98-00-0
Benzaldehyde	Aladdin Co. Ltd.	CAS: 100-52-7
Dichloromethane	Aladdin Co. Ltd.	CAS:75-09-2
Benzoic acid	Aladdin Co. Ltd.	CAS:65-85-0
β-Carotene	Aladdin Co. Ltd.	CAS:7235-35-7
p-Benzoquinone	Aladdin Co. Ltd.	CAS:106-51-4
2, 2, 6, 6-Tetramethyl-1-piperidinyloxy (TEMPO)	Aladdin Co. Ltd.	CAS: 2564-83-2
Tetra (4-carboxylphenyl) porphyrin (H_2TCPP)	Aladdin Co. Ltd.	CAS:14609-54-2
m -Tetraphenyl porphyrin (H_2TPP)	Aladdin Co. Ltd.	CAS:917-23-7
Tetraphenyl porphyrin zinc (ZnTPP)	Aladdin Co. Ltd.	CAS:14074-80-7
Ethyl acetate	Damao Chemical Reagent Factory	CAS:141-78-6
Furfural (FUR)	Damao Chemical Reagent Factory	CAS:98-01-1
N, N-dimethyl formamide (DMF)	Damao Chemical Reagent Factory	CAS:68-12-2
t-Butanol	Damao Chemical Reagent Factory	CAS: 75-65-0
Acetic acid	Macklin Co. Ltd.	CAS:64-19-7
Tetra (*p*- methylphenyl) porphyrin (H_2TMPP)	Macklin Co. Ltd.	CAS:14527-51-6
Tetra (*p*-cyanophenyl) porphyrin (H_2TCNPP)	Macklin Co. Ltd.	CAS:14609-51-9
Tetraphenyl porphyrin copper (CuTPP)	Macklin Co. Ltd.	CAS:14172-91-9
Tetra (*p*-chlorophenyl) porphyrin iron (FeTClPP)	Macklin Co. Ltd.	CAS:36965-70-5
Tetra (*p*-chlorophenyl) porphyrin manganese (MnTClPP)	Macklin Co., Ltd.	CAS: 62613-31-4
Hydrochloric acid	Tianjin Fengchuan Chemical Reagent Co.,Ltd.	CAS:7647-01-0
Acetone	Tianjin Fengchuan Chemical Reagent Co.,Ltd.	CAS:67-64-1
Dimethylsulfoxide (DMSO)	Tianjin Fengchuan Chemical Reagent Co.,Ltd.	CAS:67-68-5
Hydrogen peroxide (30%)	Tianjin Fengchuan Chemical Reagent Co.,Ltd.	CAS:7722-84-1

RESOURCE AVAILABILITY

Lead contact

Further information and requests for resources should be directed to and will be fulfilled by the lead contact, Xinli Tong (tongxinli@tju.edu.cn).

Materials availability

All materials generated in this study are available from the lead contact without restriction.

Data and code availability

The data in this article will be provided by the lead contact upon the reasonable request.

There is no any dataset and original code related to this study.

METHOD DETAILS

General information

The equipment for valuation of catalytic reaction was a 120 mL stainless -steel autoclave with a glass window and magnetic stirring. The CEL-HXF300 Xe lamp was employed as the light supply. The quantitative analysis of the products was carried out on the Agilent 8860 gas chromatograph (GC) equipped with HP-5 column and flame ion detector (FID). The conversion of the substrate and selectivity of products were calculated with the internal standard method. The Agilent 6890/5973 gas chromatography-mass spectrometry (GC-MS) and nuclear magnetic resonance spectroscopy(NMR, 500 MHz) was used to detect the structure of product.

General procedure for the photocatalytic selective oxygenation

The photocatalytic oxygenation of furanic platform compound (FAC, FUR or FAL) was performed in the autoclave with a glass window and magnetic stirring. The typical step for the transformation of FAC is as follows: 0.1 g of FAC, 0.001 g of porphyrin-based catalyst and 10 mL solvent (DMSO, acetonitrile, DMF, acetone, toluene, n-hexane, octane or ethyl acetate) are added to the steel high-pressure reactor. After the autoclave being sealed, pure oxygen (O_2) is charged to replace the inner air of the reactor. Then, the O_2 pressure is kept at about 0.3 MPa after the gas inside being exchanged for three times; in the following, the autoclave is placed under the irradiation of Xe lamp light supply. When the reaction is completed, the solution is transferred to the volumetric flask and the obtained products are detected by the Aglient GC and GC-MS instruments, respectively. In the isotope labeling experiment, the ^{18}O was used for the reaction instead of the regular $^{16}O_2$ as the oxidant.

Control experiments for detecting active oxygen species during the reaction

The control experiments are performed as follows: 0.1 g of FAC, 0.002 g of porphyrin-based catalyst, 0.1 g additive (β-carotene, p-benzoquinone, t-butanol or TEMPO) and 10 mL ethyl acetate are added to the steel high-pressure reactor. After the autoclave being sealed, pure oxygen is charged to replace the inner air of the reactor. Then, the oxygen pressure is kept at about 0.3 MPa after the gas inside being exchanged for three times; in the following, the autoclave is placed under the irradiation of Xe lamp light supply. When the reaction is completed, the solution is transferred to the volumetric flask and the obtained products are examined by the Aglient GC and GC-MS instruments, respectively.

Separation of succinic anhydride (SAN)

After the reaction finished, the mixture was distilled under the vacuum to remove the solvent, and the remaining solid products were washed several times by n-hexane; then, the crude product was recrystallized using the dichloromethane and n-hexane, and the final product SAN was obtained by vacuum drying. The structure of product was examined by the NMR technique.